RSC Advances

ROYAL SOCIETY OF CHEMISTRY

www.rsc.org/advances

Journal Name

ARTICLE

A novel cage-like CdTe film with enhanced photoelectrochemical performance

Received 00th January 20xx,
Accepted 00th January 20xx

DOI: 10.1039/x0xx00000x

www.rsc.org/

Jun Wang,[a] Pin Lv,[a] Yannan Mu,[b] Dong Ding,[a] Li Liu,[a] Runa A,[a] Fei Feng,[a] Shuang Feng,[a] Wuyou Fu,[a] and Haibin Yang*[a]

A novel cage-like CdTe film with even porosity size and good connectivity among particles is successfully prepared by a simple technique for the first time. The field emission scanning electron microscopy (FESEM), X-ray diffraction (XRD) and UV-Vis absorption spectra are used to characterize the morphology, crystallinity and optical property of the new structure. The FESEM observation confirms the formation of cage-like CdTe film after heat treatment. The structural and optical studies reveal that the cage-like CdTe films show better crystallinity and enhanced optical absorption. Based on the characterization results, the possible growth mechanism of the cage-like CdTe film is proposed. Furthermore, the photoelectrochemical property of the film is also investigated by photocurrent and current density–voltage curves and electrochemical impedance spectroscopy (EIS). The cage-like CdTe film yields an enhanced photocurrent and current density of 3.8 mA cm^{-2}, which is significantly higher than other as-prepared CdTe films. Meanwhile, the cage-like CdTe films present improved charge transfer properties and corroborate the photocurrent and current density–voltage measurements. The photostability of the films is also studied. The better photoelectrochemical property of the cage-like CdTe films suggests their potential application in nanostructured solar energy conversion devices.

Introduction

Solar power is a promising candidate as a sustainable energy supply. During the last decade, the increasing interest in the applications of solar cells has led to intensive research on the development of inexpensive materials and architectures that reduce cost and/or increase efficiency.[1]

As a direct band gap semiconductor with high atomic number and electron density, CdTe has been widely used in applications of photovoltaics, sensors, and detectors.[2–4] With its narrow and direct band gap (Eg = 1.45 eV), stability, and other optoelectronic and photoelectrochemical properties, in recent years, it has been suggested that CdTe nanostructures can serve as functional building blocks for optoelectronic and photovoltaic nanodevices,[5–7] and is a crucial aspect of increasing the current energy conversion efficiency of solar cell.[8–16] The synthesis and assembly of CdTe with different forms of controlled nanostructures have been widely explored in recent years and many kinds of interesting and delicate CdTe nanostructures have been obtained by using different methods.[17–21] Among the numerous methods, it is generally admitted that electrodeposition is an attractive method for preparation of CdTe thin films in commercial quantities because of the low fabrication costs, facile control of film thickness, morphology and doping concentration through applied potential, current, pH and temperature of the bath.[22–25] Therefore, more and more researchers are concentrating on electrochemical deposition to fabricate patterned vertically aligned CdTe. For instance, vertically aligned CdTe nanotubes have been deposited on ITO glass in large scale by using ZnO nanorod arrays as templates.[26] The CdTe nanorods also have been obtained by using anodic aluminum oxide as template, forming the array configuration.[27] However, both of the hard and the soft template-assisted synthesis methods usually require high-cost and tedious procedures, including template modification, precursor attachment, and core removal. For that reason, many efforts have been made to give insight into the fabrication of the CdTe thin film without any templates. It is widely accepted that another common method of shape control is to select an appropriate additive, leading to the morphological modification of the crystals. For example, in our previous work, sodium chloride (NaCl) is added into the electrolyte directly, and an interesting morphology evolution has been observed.[28] The increase of NaCl concentration can enhance the CdTe deposition efficiency, resulting in an enhancement of the longitudinal growth rate. However, the excessively long length of the CdTe nanorod can result in loss of adhesion, and the film can easily peel off from the Ni substrate. Similar phenomena may occur in the electrodeposition of ZnO film with the addition of NaCl.[29] So, it is still a great challenge to develop low-cost, environmentally friendly, simple, and versatile approaches for synthesis of

[a] State Key Laboratory of Superhard Materials, Jilin University, Qianjin Street 2699,Changchun, 130012, People's Republic of China; Fax: +86 431 85168763; Tel: +86 431 85168763; E-mail:yanghb@ jlu.edu.cn
[b] Department of Physics and Chemistry, Heihe University, Heihe 164300, PR China

nanostructures that will greatly facilitate the future application of structures in various fields.

It is generally known that the chemical activities of the materials are related to their morphologies, and the shapes are directly related to their properties and stabilities. So the development of nano-materials of a specific size and with defined shape has attracted great interests in recent years. Many efforts have focused on the formation of one-dimensional nanostructures due to their special physicochemical properties as well as their potential technological applications in nano-devices such as nanowires,[30] nanorods,[31] nanotubes,[32] *etc*. In fact, in addition to these common architectures, hollow spheres represent an important class of materials and have received significant attention because of their unique structural characteristics, special physicochemical properties as well as their potential technological applications in nano-devices. Many efforts have focused on the formation of various materials with hollow nanostructures. For instance, Ping and his co-workers report a cage-like nano-$CaCO_3$ hollow spheres with different cavity sizes prepared using the template-directed synthesis method. Ibupoto *et al*. present a cage-like NiO nanostructures prepared by hydrothermal growth method. Shen *et al*. fabricate a novel hollow ZnO urchin by thermal evaporation.[33–35] The highly crystalline hollow nanostructures with various sizes and morphologies have been widely applied in different fields due to their low effective density, high specific surface area, better permeation, intriguing size- and shape-dependent properties. Nevertheless, as far as we know, there are no reports about hollow CdTe nanostructures because controlled organization of primary building units into curved structures represents another challenge for materials self assembly. Thus, the synthesis of hollow CdTe thin films is of remarkable interest and challenge.

In this paper, we first present a simple method to realize large scale synthesis of cage-like CdTe with well-distributed holes, better connectedness and high crystallinity on a Ni substrate without use of any additive, high temperature, or template. Detailed characterization of the sample morphology and structure is performed. The absorption spectra and EIS are used to investigate the optical and photoelectrochemical properties of the film. We find that the cage-like CdTe films exhibit enhanced optical absorption. Meanwhile, EIS test result also shows that the cage-like CdTe films have relatively small impedance. These improvements above lead to a significantly enhanced photoelectrochemical properties of the film, indicating its possible potential application in nano-structured solar energy conversion devices.

2. Experimental

2.1 Preparation of cage-like CdTe film

Firstly, the CdTe nanorod array film is fabricated using a rapid and convenient electrodeposition method. The electrochemical experiments are carried out in a three electrode electrochemical cell. Prior to electrodeposition, the Ni substrates and graphite plate are pretreated with acetone and ethanol in turn and then rinsed thoroughly with deionized water prior to each deposition. The electrolyte is prepared by dissolving 0.001 mol L^{-1} $CdSO_4$• 8/3 H_2O in 0.005 mol L^{-1} Na_2TeO_3 solution, and is further adjusted to pH = 2 with H_2SO_4. All of the chemicals are of analytical grade and used without further purification. The rod-like CdTe films are synthesized at a fixed potential of –0.5 V (vs. Ag |AgCl |KCl (sat)). After deposition, the rod-like CdTe films are thoroughly washed with distilled water, and then are annealed at different temperature in nitrogen (N_2) atmosphere for 0.5 h to form cage-like structures. Finally, the cage-like CdTe film is obtained by annealing the rod-like CdTe film at 400℃. The effect of annealing temperatures on the morphology of CdTe is further discussed. It is worth mentioning that the whole synthesis is performed without use of any surfactant or capping agent.

2.2 Characterization

The morphology of the products is characterized by means of field emission scanning electron microscope (FESEM, JEOL JSM-6700F). The structure is investigated via a Rigaku D/max-2500 X-ray diffractometer (XRD) with Cu Kα radiation (λ = 1.5418 Å), in the scanning range between 20° and 80°. UV-Vis absorption is recorded in the range from 300 to 1000 nm by UV-3150 double-beam spectrophotometer at room temperature. All the electrochemical tests are performed in a quartz cell using standard three-electrode configuration. The as-synthesized CdTe film is used as the working electrode, Pt wire as the counter electrode, and Ag |AgCl |KCl (sat) as the reference electrode. The electrolyte is a mixture of 0.25 mol L^{-1} Na_2S and 0.35 mol L^{-1} Na_2SO_3 aqueous solution. Photoelectrochemical performance is measured by a CHI601C electrochemical workstation under a xenon lamp with power of 500 W and intensity of 100 mW cm^{-2}. To measure the electron behaviors, the electrochemical impedance spectroscopy (EIS) measurements are carried out by a CHI601E electrochemical workstation at the open circuit potential (–0.5 V). In addition, to further investigate the photostability of all the as-prepared thin films, the photostability measurement is performed and the variations of the photocurrent and current with time, are measured under a simulated one sun illumination (100 mW cm^{-2}) at 0 V (vs. Ag |AgCl |KCl (sat)). All the electrochemical measurements are carried out at room temperature (25 ± 2 ◦C).

3. Results and discussion

3.1 Morphology and structure

The morphology and crystal structure of the rod-like CdTe film and the cage-like CdTe film are confirmed by FESEM and XRD, as shown in Fig. 1. Fig. 1A shows that the rod-like CdTe film with a smooth surface formed after electrodeposition. When the film is annealed at 400 ℃, it is found that the as-prepared CdTe films (Fig. 1B) possess a cage-like structure. On further inspection by means of a high-magnification SEM image (Fig. 1C), the cage-like surfaces are made up of interconnected nanoparticles from 80 nm to 100 nm in size suggesting that the cage-like CdTe nanostructures have even porosity size and

good connectivity. In addition, the cage-like CdTe array films remain a rod-like shape. More structure details of the cage-like film are further elucidated by the XRD result, as shown in Fig. 1D. It can be seen that besides the Ni substrate and Te-Ni compound peaks generated by the reaction between CdTe and Ni, the main diffraction peaks at 2θ values for 23.98°, 39.70° and 49.90° correspond to the (111), (220) and (311) planes of zinc-blende CdTe, as confirmed by the JCPDS X-ray powder file data (Data file 75-2086).[36] XRD patterns show that the pure rod-like CdTe has an amorphous structure (Fig. 1D (a)), while the sharp diffraction peaks indicate that the cage-like CdTe film is well crystallized, as shown in (Fig. 1D (b)). No other diffraction peaks are observed for impurities such as CdO, TeO_x or $CdTe_yO_x$, indicating the high purity of the products, while Te-Ni compound is generally used as an ohmic contact layer which can reduce the contact resistance between metal (Ni) and semiconductor (CdTe) thus improve the charge mobility.

In order to investigate the effect of experiment parameters on the morphology and the evolution process of the cage-like CdTe film in more detail, experiments are carried out at different annealing temperatures from 300 ℃ to 450 ℃ for 0.5 h, and the results revealed that the annealing temperatures play a key role in the formation of the cage-like structure. Fig. 2 presents the typical SEM images of the samples annealed at different temperatures and the evolving process can be distinctly observed. As shown in Fig. 2A, the morphology exhibits no obvious difference after annealing at 300 ℃. It is noteworthy that it still remains a well-connected and uniform rod-like morphology. When the film is annealed at 350 ℃ (Fig. 2B), the surface of the rod becomes coarse. A small number of holes with small size appear on the surface of the CdTe nanorod. When the temperature is further increased to 400 ℃ (Fig. 2C), a big change in the shape and size of the CdTe films is observed. Some pores appear and the cage-like CdTe film is fabricated. As can be seen in Fig. 2C, the number and diameter of holes increase. The film exhibits better connectivity between particles. Fig. 2D exhibits the morphology of the sample which is obtained at 450 ℃. Holes get even more and bigger after heat treatment. It can be

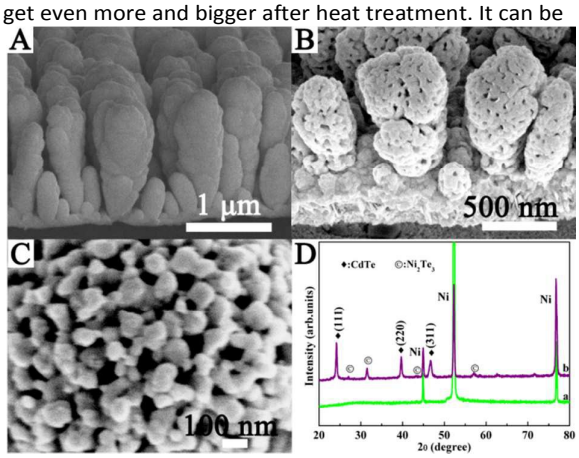

Fig. 1 (A) Low-magnification SEM image of rod-like CdTe film, (B) Low-magnification SEM image of cage-like CdTe film, (C) high-magnification SEM image of cage-like CdTe film and (D) XRD patterns of (a) the rod-like and (b) cage-like CdTe film.

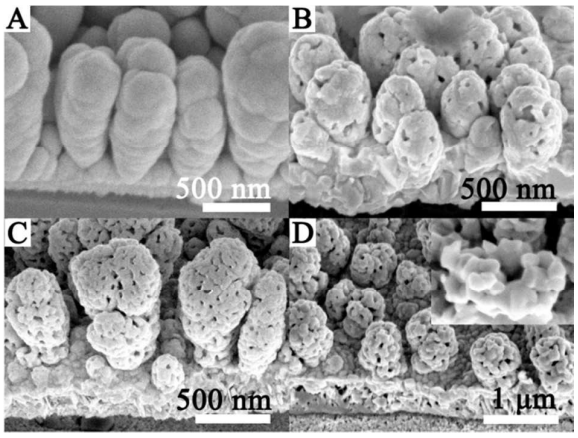

Fig. 2 SEM images of CdTe films annealed at different temperature: (A) 300 ℃, (B) 350 ℃, (C) 400 ℃ and (D) 450 ℃, respectively.

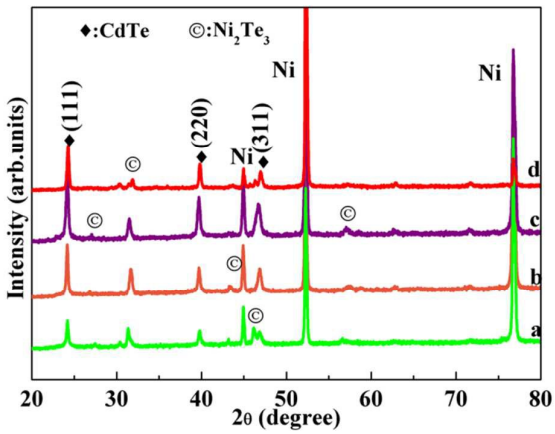

Fig. 3 XRD patterns of CdTe films annealed at different temperature: (a) 300 ℃, (b) 350 ℃, (c) 400 ℃ and (d) 450 ℃, respectively.

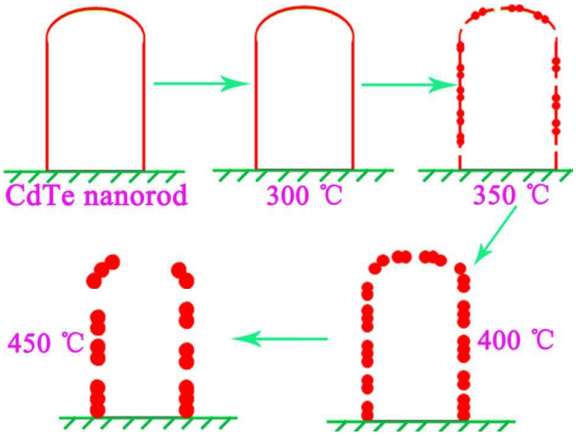

Fig. 4 Schematic diagram of the possible formation mechanism of the cage-like CdTe film.

observed that the cage-like structure is broken into some parts forming a larger hole or some vacancies. The inset in Fig. 2D shows the high-magnification image of the structure. These results confirm that the annealing temperatures play a very

important role in forming the cage-like CdTe architecture. It is obviously that the number of holes increases as the annealed temperature increases. Meanwhile, the porosity size also increases with increasing the annealing temperature. Therefore, in order to obtain a uniform cage-like CdTe architecture, the as-deposited CdTe thin film should be annealed at 400 ℃ for 0.5 h.

Fig. 3 shows the XRD patterns of CdTe films after heat treatment at different temperature. It can be seen that all the diffractions can be indexed to the zinc-blende CdTe and the intensive reflections reveal the highly crystalline nature of the product after heat treatment. What's more, in all cases, the intensities of the (220) and (311) peaks are quite low as compared to that of the (111) one. This result indicates a preferential orientation of the products with the (111) plane perpendicular to the substrate, which is similar to the previous reports.[37–39] For the samples annealed at different temperatures, it is worthwhile to note that with the annealing temperature increasing, the intensity of CdTe (111) peak initially increases, and then decreases, indicating that the annealing temperatures significantly affect the crystalline quality of CdTe films. This phenomenon can be also observed from reference paper.[40] The cage-like CdTe film annealed at 400 ℃ shows maximum diffraction intension to (111) plane in comparison with the others, indicating the best crystallinity among these films. When the annealing temperature is above 400 ℃, the films show their poor structure, leading to their poor crystallinity. This phenomenon can be explained that, at the beginning, with the increase of the annealing temperature, the densities of crystallographic defects in the CdTe films decrease rapidly forming the best structural property of CdTe thin films with good connectivity. But the rising temperatures will have a great influence on the structure of the film. As is shown in Fig. 2, the higher the temperature, the more holes can be formed. As a result, it caused the poor connectivity of the film, leading to poor crystallization. Besides, after the very careful analysis of the XRD patterns, it can be seen that the CdTe films have approximately the same crystallinity after annealing respectively at 350 ℃ and 450 ℃. It is a useful result to demonstrate that the structure is a dominating factor leading to enhanced photoelectrochemical performance.

3.2. Growth mechanism

Based on the above experimental results, a possible formation mechanism of the cage-like CdTe film is proposed here, and for simplicity, the growth mechanism is presented with a schematic diagram shown in Fig. 4. Electrodeposition is a simple method to synthesize the rod-like structure of CdTe. As we all know, the formation of nanocrystals in the reaction solution is generally divided into nucleation and growth processes. In the initial stage of reaction, small CdTe particles are formed on the surface of Ni foil. Because of the structural anisotropy and surface electric polarity of CdTe, the growth rates along crystal direction [111] prior to the other crystal directions. As a result, CdTe nanorods grew along [111] direction spread on the substrate. The annealing processing, as it is commonly known, significantly affects the crystal structure.[41] Thus, our research provides further observations on annealed thin films. In order to further investigate the effects of heat treatment on the microstructure, a detailed analysis for the CdTe films annealed at different temperatures is carried out. A clear change in crystallographic orientation occurred due to the annealing process. Because of crystallization, the structure of annealed CdTe has a strong preferential orientation of the (111) planes perpendicular to the substrate, whereas other peaks are weak. This phenomenon can be explained as follows: the crystallization process during annealing has two stages, in the beginning, the crystallization is dominated by random orientation of the grains followed by a second process in which once again the crystallites tend to orient in a particular direction.[42] Planes tend to be random annealed at lower temperatures, and the orientation of planes tends to obtain the specific direction with increasing the annealing temperature. The above mentioned results are in perfect agreement with the X-ray diffraction patterns. As one can see from Fig. 2, it can be concluded that heat treatment also has a great influence on the morphology of the CdTe products. It appears that the heat treatment crystallizes the CdTe layers in such a way that some of the small grains coalesce together while some of the bigger grains divide into small grains and connect with each other through the oriented attachment process,[43] and thus the cage-like structure is formed. Therefore, surface morphology exhibits more well-connected and uniform cage-like nanostructure after annealing at 400 ℃; however, some vacancies are generated after annealing at 450 ℃. Such phenomenon of morphology changes could be ascribed to that fact that annealing increases atomic mobility and improve the ability of atoms to find the most energetically favored sites. With increasing the annealing temperature, atomic mobility increases, and the Cd and Te atoms involved combine to form a new structure at appropriate temperatures. However, at a higher annealing temperature, atoms move too fast to retain the integrity of the structure, causing the entire structure to be destroyed at last. On the basis of the above discussion, we can conclude that annealing temperature is the critical parameter for the formation of cage-like CdTe film.

3.3. Optical properties and photoelectrochemical activity

For the application of the CdTe in photovoltaic devices, their optical absorption properties are fundamentally important for the performance of the devices. To investigate the influence of heat treatment on the optical property of CdTe, UV-Vis spectra collected from the formed CdTe samples are recorded in the wavelength range of 300-1000 nm and the obtained spectra have been presented in Fig. 5. It can be observed from Fig. 5 that all the samples exhibit prominent absorption in the visible region. In comparison to the CdTe sample annealed at low temperature, obvious increase in absorbance of films has been observed as the temperature raising. We think the main factor contributing to the significant increase of absorption is the enhanced crystallization performance. Another factor contributing to the increase of absorption is the elevated roughness of the CdTe relative to that of CdTe nanorod array

with smooth surface, which can capture more light and get higher light to electric efficiency. Obviously, among all of the films, the cage-like CdTe films exhibit the highest absorptivity. Several factors may be accountable for the strongest visible light absorption performance of the cage-like CdTe films. Firstly, the cage-like CdTe films have the best crystal quality among these products. Secondly, it is well known that, as the size of particles increases, the scattering intensity increases. As is shown in Fig. 2, with increasing the annealing temperature, the cage-like structure has appropriate particle size and good connectivity among particles, which can be attributed to an increase in light scattering in the arrays. However, the scattering intensity decreases for CdTe annealed at 450 ℃. This may be ascribed to its poor structure after treatment at higher temperature. The uniform arrays have been destroyed after heat treatment. Based on the above, one can draw a conclusion that the proper heat treatment temperatures not only lead to the better crystallinity but also improve the optical absorption ability, which means that more photons can be absorbed and utilized for generating photocurrent. Experiments also led to the conclusions that the light absorption has a lot to do with the morphology of the films, especially for the cage-like CdTe film. Among all the samples, the cage-like CdTe film has the best light absorption because of its fine size of particles, and perfect connectivity between pores.

The photocurrent and current curves of CdTe films annealed at different temperature under dark and illuminated conditions, respectively, are illustrated in Fig. 6. We use a conventional three-electrode system made of quartz cell linked with the electrochemical workstation, which is composed of the as-prepared samples as a working electrode, a Pt wire as a counter electrode and a saturated Ag |AgCl |KCl (sat) as a reference electrode. The electrolyte solution consists of 0.25 mol L^{-1} Na_2S and 0.35 mol L^{-1} Na_2SO_3. This polysulfide redox mediator is known to form charge separating junctions with CdTe.[44] When the sample is irradiated under simulated 100 mW cm^{-2} illumination, it can absorb more light, and generate more electron–hole pairs at the interface between the sample and the polysulfide electrolyte. As a result, more electron–hole pairs would separate in the space charge region. Electrons are concentrated into the center of the film deposited on the Ni substrate to be transported, and holes are transferred to the polysulfide redox electrolyte solution. A closed circuit is formed and finally the current density versus voltage characteristic of different samples is measured via computers under dark and illumination conditions respectively, as shown in Fig. 6. Under dark conditions, the observed dark current densities for the CdTe films annealed at different temperature can be negligible (Fig. 6 (e-h)). The four photocurrent and current curves of CdTe films annealed at different temperature in the dark overlap together. Under illumination, all photocurrents show outstanding enhancements compared to the dark currents due to the light response of the electrodes. Besides, as we can see from Fig. 6, we find that the heat treatment seems to have no significant influence on the open circuit photopotential of the samples. However, a remarkable difference in the current density is observed and it clearly shows that the current

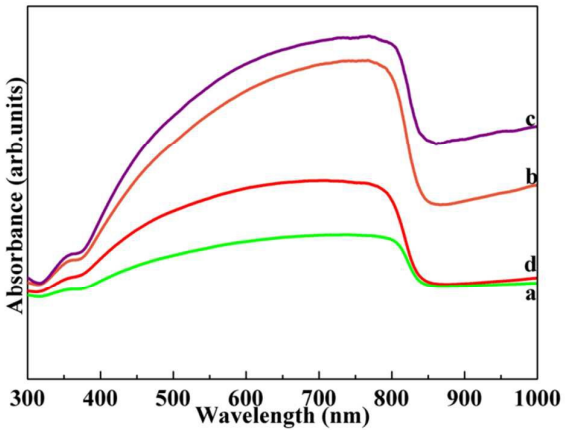

Fig. 5 UV-Vis absorption spectra of CdTe films annealed at different temperature: (a) 300 ℃, (b) 350 ℃, (c) 400 ℃ and (d) 450 ℃, respectively.

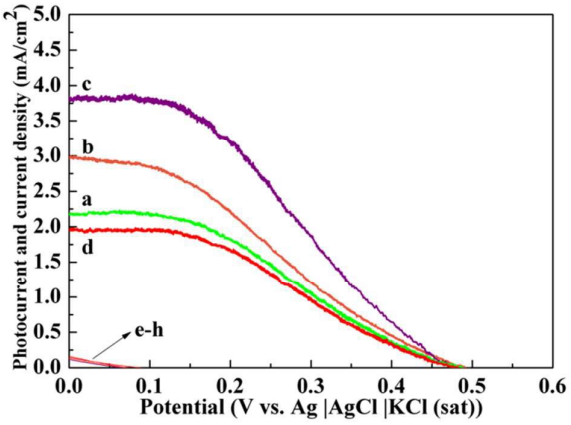

Fig. 6 Photocurrent and current curves of CdTe films annealed at different temperature: (a) 300 ℃, (b) 350 ℃, (c) 400 ℃, and (d) 450 ℃ under illumination; (e-h) Four photocurrent and current curves of CdTe films annealed at different temperature in the dark.

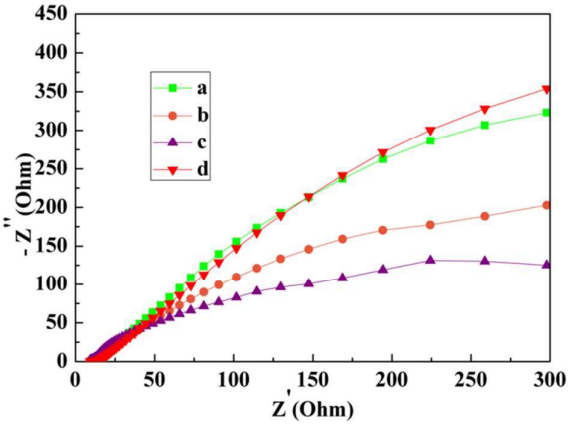

Fig. 7 Electrochemical impedance spectra of CdTe films annealed at different temperature: (a) 300 ℃, (b) 350 ℃, (c) 400 ℃ and (d) 450 ℃, respectively.

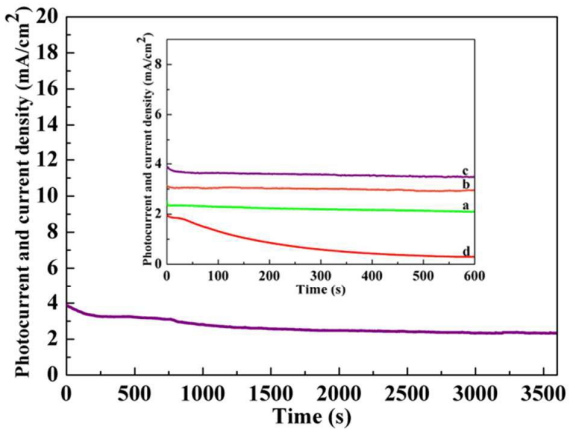

Fig. 8 Long term photostability of cage-like CdTe films for 3600 s. The inset shows the photostability of CdTe films annealed at different temperature: (a) 300 ℃, (b) 350 ℃, (c) 400 ℃ and (d) 450 ℃ for 600 s.

density exhibits an interesting trend under illumination, namely, firstly increase and reach a maximum, and then decrease with the annealing temperature. It can be seen that cage-like CdTe films exhibit the best photocurrent and current density of 3.8 mA cm^{-2}. The photocurrent and current (3.8 mA cm^{-2}) is higher than our previous reports.[28] However, as seen from the results of photocurrent and current curves, there is still much room for improvement. Several factors may be responsible for the best photochemistry performance of the cage-like CdTe film. Firstly, the cage-like CdTe film has better crystal quality, which is beneficial for electronic transmissions. Secondly, as is shown in Fig. 1, the sample with highly uniform morphologies may have significant photoabsorption, and the enhancement of optical absorption can be attributed to an increase of light scattering in the arrays constituted by highly uniform structure, which is consistent with the UV-Visible absorption spectrum (Fig. 5). What's more, the remarkable photoabsorption capacity of the cage-like CdTe is a direct result of the generation of charge carriers. Thirdly, as can be seen in Fig. 2C, cage-like CdTe array films remain a rod-like pathway, which can ensure the photogenerated electrons to travel along the longitudinal direction of rods with minimum loss. Finally, the cage-like CdTe morphology can obtain a better contact with the electrolyte, which improves the efficiency of charge separation and charge extraction, indicating that this kind of cage-like morphology might be detrimental for use in photovoltaic devices. In contrast, it is also to be noted that the photocurrent and current decreases, when the film is annealed at 450 ℃. In contrast with the film annealed at 350 ℃ with approximately the same crystallinity, this behaviour can be attributed to its poor morphology, which causes a recombination of charge carriers at the grain boundaries of the film. These grain boundaries can act as a potential barrier, enhance the possibilities of the recombination between electrons and holes, and prevent the change transfer, leading to a decrease in the overall efficiency. To elucidate the underlying mechanism of morphology related to the interface charge transfer, EIS is performed for all the samples annealed at different temperature. In Nyquist curves shown in Fig. 7, the cage-like CdTe films have minimum semicircle diameters, indicating that it has best electrical conductivity, which is favor of photogenerated electrons transport to the collecting electrode (Ni substrate foil). In addition, this observation by EIS is supporting clearly why the morphology of the CdTe film is very important for improving photovoltaic performances (Fig. 6). Therefore, we think, in this paper, the structure is essential to the efficient photovoltaic performance of CdTe films. The photostability profile of the as-prepared CdTe films is also investigated. The photocurrent and current curves of CdTe films are measured at a certain time, while the films are exposed to continuous light illumination. The long-term photostability of cage-like CdTe films is measured at 0 V (vs. Ag |AgCl |KCl (sat)) under continuous light illumination of 1 h, as shown in Fig. 8. It should be noted that the cage-like CdTe films do not show a significant degradation after continuous sunlight illumination for 1 h. For a clear comparison of the photostability, the photostability of CdTe films annealed at different temperature is also investigated for 600 s (as shown in the inset in Fig. 8). After careful analysis, it can be found that, among all of the films, the cage-like CdTe films exhibit better photocurrent and current behaviour than other shaped CdTe films leading to comparatively lesser degradation in photocurrent and current (Fig. 8(c)). The photocurrent and current of the film annealed at 450 ℃, on the contrary, exhibits severe degradation than the other products (Fig. 8(d)) during constant light illumination of 600s. The obvious drop of photocurrent and current may be attributed to its poor structure. This result also suggests that the structure plays a key role in determining the photostability. Furthermore, based on the above, one can draw a conclusion that the cage-like CdTe films are stable in chemical properties and show good photostability. The improved photoelectrochemical performance of the annealed CdTe films indicates their potential for application in thin-film solar cells.

Conclusions

In summary, this paper puts forward a simple, template-free electrochemical synthesis method to fabricate a novel cage-like CdTe film for the first time. We successfully capture the suitable condition for the formation of a cage-like structure by controlling the experiments, and a combined growth mechanism is proposed for the formation of this novel structure. This novel cage-like CdTe film has even porosity size and good connectivity among particles. The films have a cubic zinc-blende structure with a strong preferred orientation along [1 1 1] direction. What's more, in contrast with other samples, the cage-like CdTe films exhibit significantly enhanced light absorption, good electron transfer ability, and the best photoelectrochemical behaviour. The higher photocurrent and current is expected to make the cage-like CdTe films more suitable for solar energy applications. Moreover, the prepared cage-like CdTe films also demonstrate good photostability in the photoelectrochemical properties for a longtime illumination. More importantly than all of that, the finding

reveals the formation mechanism of the cage-like CdTe thin film, which may serve as one of the typical growth mechanisms for the cage-like structure and prove helpful for understanding and controlling the growth behaviour of cage-like structures. The synthetic strategy presented here provides a very facile route for preparing novel structures by heat treatment of shaped CdTe film in future research.

Acknowledgements

This work was financially supported by National Natural Science Foundation of China (No. 51272086), the Technology Development Program of Jilin Province (Grant no. 20100417) and Graduate Innovation Fund of Jilin University (No. 2015106).

References

1 L. E. Greene, M. Law, B. D. Yuhas and P. D. Yang, J. Phys. Chem. C, 2007, **111**, 18451–18456.
2 I. Visoly-Fisher, S. R. Cohen, A. Ruzin and D. Cahen, Adv. Mater., 2004, **16**, 879–883.
3 N. N. Mamedova, N. A. Kotov, A. L. Rogach and J. Studer, Nano Lett., 2001, **1**, 281–286.
4 J. Kang, E. I. Parsai, D. Albin, V. G. Karpov and D. Shvydka, Appl. Phys. Lett., 2008, **93**, 223507.
5 A. R. Flores., R. Castro-Rodrı'guez, J. L. Pena, N. Romeo and A. Bosio, Appl. Surf. Sci., 2009, **255**, 7012–7016.
6 X. Wang, Y. M. Xu, H. J. Zhu, R. Liu, H. Wang and Q. Li, CrystEngComm, 2011, **13**, 2955–2959.
7 Y. L. Li, L. H. Jing, R. R. Qiao and M. Y. Gao, Chem. Commun., 2011, **47**, 9293–9311.
8 B. W. Luo, Y. Deng, Y. Wang, M. Tan, L. L. Cao and W. Zhu, CrystEngComm, 2012, **14**, 7922–7928.
9 B. M. Basol, Sol. Energy Mater. Sol. Cells, 1988, **23**, 69–88.
10 A. Shah, P. Torres, R. Tscharner, N. Wyrsch and H. Keppner, Science, 1999, **285**, 692–698.
11 E. I. Parsai, D. Shvydka and J. Kang, Med. Phys., 2010, **37,** 3980.
12 R. L. Yang, D. Z. Wang, L. Wan and D. l. Wang, RSC Adv., 2014, **4**, 22162–22171.
13 J. Britt and C. Ferekides, Appl. Phys. Lett., 1993, **62**, 2851–2852.
14 H. Ohyama, Proc. of 26th IEEE PVSC, 1997, 343–346.
15 D. Cunningham, Proc. of 28th IEEE PVSC, 2000, 13–18.
16 T. Aramoto, Proc. of 28th IEEE PVSC, 2000, 436–439.
17 J. L. Plaza, O. Martínez, S. Rubio, V. Hortelanob and E. Diégueza, CrystEngComm, 2013, **15**, 2314–2318.
18 E. R. Shaaban, N. Afify and A. El-Taher, J. Alloys Compd., 2009, **482**, 400–404.
19 Y. M. Sung, W. C. Kwak and T. G. Kim, CrystEngComm, 2012, **14**, 389–392.
20 P. Ramasamy, S. I. Mamum, J. Jang and J. Kim, CrystEngComm, 2013, **15**, 2061–2066.
21 S. Ham, B. Choi, N. Myung, N. R. de Tacconi, C. R. Chenthamarakshan, K. Rajeshwar and Y. Son, J. Electroanal. Chem., 2007, **601**, 77–82.
22 Q. Li, L. C. Tian, K. L. Chi, H. B. Yang, M. L. Sun and W. Y. Fu, Appl. Surf. Sci., 2013, **270**, 707–711.
23 N. W. Duffy, D. Lane, M. E. OÈ zsan, L. M. Peter, K. D. Rogers and R. L. Wang, Thin Solid Films, 2000, **361**, 314–320.
24 L. C Tian, J. Ding, W. Zhang, H. B. Yang, W. Y. Fu, X. M. Zhou, W. Y. Zhao, L. N. Zhang and X. Y. Fan, Appl. Surf. Sci., 2011, **257**, 10535–10538.
25 A. Jarkov, S. Bereznev, O. Volobujeva, R. Traksmaa, A. Tverjanovich, A. Öpik and E. Mellikov, Thin Solid Films, 2013, **535**, 198–201.
26 X. N. Wang, H. J. Zhu and Y. M. Xu, ACS Nano, 2010, **4**, 3302–3308.
27 Y. M. Sung, W. C. Kwak and T. G. Kim, CrystEngComm, 2012, **14**, 389–392.
28 J. Wang, Q. Li, Y. N. Mu, X. M. Zhou, L. H. Yang, P. Lv, S. Su, J. S. Niu, W. Y. Fu and H. B. Yang, RSC Adv., 2015, **5**, 43016–43022.
29 R. Tena-Zaera, J. Elias, G. Wang, and C. Le´vy-Cle´ment, J. Phys. Chem. C, 2007, **111**, 16706–16711.
30 N. S. Lewis, Science, 2007, **315**, 798–801.
31 R. F. Service, Science, 2008, **319**, 718–720.
32 K. M. Coakley and M. D. McGehee, Chem. Mater., 2004, **16**, 4533–4542.
33 G. Z. Shen, Y. Bando and C. J. Lee, J. Phys. Chem. B, 2005, **109**, 10578–10583.
34 Z. H. Ibupoto, A. Nafady, R. A. Soomro, Sirajuddin, S. T. H. Sherazi, M. I. Abro and M. Willander, RSC Adv., 2015, **5**, 18773–18781.
35 H. L. Ping and S. F. Wu, RSC Adv., 2015, **5**, 65052–65057.
36 W.H. Zachariasen, Nor.Geol.Tidsskr., 1926, **8**, 302.
37 M. E. Calixto, J. C. McClure, V. P. Singh, A. Bronson, P. J. Sebastian and X. Mathew, Sol. Energy Mater. Sol. Cells, 2000, **63**, 325–334.
38 G. P. Hernandez, X. Mathew, J. P. Enriquez, N. R. Mathews and P. J. Sebastian, Sol. Energy Mater. Sol. Cells, 2001, **70**, 269–275.
39 S. Y. Yang , J. C. Chou and H. Y. Ueng, Thin Solid Films, 2010, **518**, 4197–4202.
40 A. Romeo, D. L. Batzner, H. Zogg and A. N. Tiwari, Thin Solid Films, 2000, **361**, 420–425.
41 B. Qi, D. Kim, D. L. Williamson and J. U. Trefny, J. Electrochem. Soc., 1996, **143**, 517–523.
42 S. Y. Yang, J. C. Chou and H. Y. ueng, Thin solid films, 2010, **518**, 4197–4202.
43 Y. Zhu, W. Zhao, H. Chen and J. Shi, J. Phys. Chem. C, 2007, **111**, 5281–5285.
44 M. Schierhorn, S.W. Boettcher and A. Ivanovskaya, J. Phys. Chem. C, 2008, **112**, 8516–8520.